

**Award Account**

Lectureship Award in Asian International Symposium for 2017

**Light and Matter Interaction in Two-Dimensional Atomically Thin Films****Rajesh Kumar Ulaganathan,<sup>1,#</sup> Yi-Hsuan Chang,<sup>2,#</sup> Di-Yan Wang,<sup>2</sup> and Shao-Sian Li<sup>\*3</sup>**<sup>1</sup>Department of Materials Science and Engineering, National Taiwan University, No. 1, Sec. 4, Roosevelt Rd., Taipei 10617, Taiwan<sup>2</sup>Department of Chemistry, Tunghai University, No. 1727, Sec. 4, Taiwan Boulevard, Xitun District, Taichung 40704, Taiwan<sup>3</sup>Graduate Institute of Biomedical Optomechatronics, Taipei Medical University, No. 250, Wuxing St., Taipei 11031, Taiwan

E-mail: ssli@tmu.edu.tw

Received: January 17, 2018; Accepted: February 4, 2018; Web Released: February 21, 2018

**Rajesh Kumar Ulaganathan**

Rajesh Kumar Ulaganathan completed his doctorate in the Department of Chemistry, National Taiwan University (2016). After his doctoral degree, he is continuing his research interest as a Post Doctorate Fellow in Material Science & Engineering Department in National Taiwan University. His current research interests are fabrication of two dimensional based crystals and perovskites materials for optoelectronic applications include transistors, photodetectors, light emitting devices, solar cells and he is also working on bio sensing using nanowires and nanosheets.

**Yi-Hsuan Chang**

Yi-Hsuan Chang received her Bachelor's degree under the supervision of Prof. Di-Yan Wang from the Department of Chemistry, Tunghai University. Her research interests include the synthesis of different metal nanomaterials used for CO<sub>2</sub> reduction reaction. She recently focuses on the self-assembly of metal nanoparticle as active matrix to improve the sensitivity of detection limit in SALDI-TOF MS.

**Di-Yan Wang**

Dr. Di-Yan Wang is currently an Assistant Professor in the Department of Chemistry, Tunghai University, a position he has held since 2016. Dr. Wang received his Ph. D. degree in chemistry from National Taiwan Normal University in 2010. Later, He was a postdoctoral fellow at the Department of Materials Science and Engineering at National Taiwan University during 2010–2013. After that, He also was a visiting scholar in the Department of Chemistry, Stanford University during 2013 to 2015. His research focuses on developing new type 2D materials for catalytic activity, photo energy and battery application fields and investigating related reaction mechanism by using operando synchrotron and Raman techniques.

**Shao-Sian Li [Award recipient]**

Dr. Shao-Sian Li is currently an Asst. Professor in the Graduate Institute of Biomedical Optomechatronics, Taipei Medical University. He received his Ph. D. degree from the Department of Materials Science and Engineering, National Taiwan University in 2011. He was a postdoctoral fellow (2014–2016), and a research scholar at National Taiwan University (2016–2017) He was also a guest research scholar at National Institute for Materials Science, Japan (2016–2017). His research focuses on the development of a platform based on two-dimensional materials for energy conversion devices and bio-sensing devices. He also works on the study of photo-carrier dynamics by optical and electrical transient measurements in correlation to the material properties.

## Abstract

Atomically thin two-dimensional (2D) materials have been a famous and fascinating material in recent years due to the potential to replace conventional semiconducting bulk electronic materials. To control the performance of 2D materials, many methods have been proposed, including physical and chemical ways, to manipulate the electronic, atomic and microscopic properties. In this work, we would like to present a physical method based on the interactions of 2D materials with light to influence the 2D material properties and device performance. By reviewing some recent published work, we will show how effective the light can be to functionalize 2D materials. The fundamental fluorescence phenomenon and current applications using 2D materials in optoelectronics, such as photodetectors, solar cells and light emitting diodes, to obtain improved device properties will also be discussed.

**Keywords:** Two-dimensional material | Graphene oxide | Perovskite solar cell

## 1. Introduction

Two-dimensional (2D) materials, possessing atomic or molecular thickness and infinite planar length, have a lot of fascinating material properties which creates tremendous research interests.<sup>1–5</sup> For example, graphene, carbon atoms arranged in honeycomb lattice structure, exhibit a linear dispersion relation near the Dirac point and cause electrons and holes to be massless, resulting in extremely high mobility.<sup>6</sup> In addition, single layer graphene has a very high optical transparency with 97.7% transmittance from visible to near infrared light.<sup>7</sup> Semiconducting transition metal dichalcogenides (TMD) are another type of 2D material that widely attracted attention due to the moderate bandgap of about 1–2 eV in comparison to gapless graphene, being considered as more ideal candidates for making low-power-consuming 2D transistors along with good carrier mobility.<sup>8</sup> High  $\kappa$  2D metal oxide materials also exhibit excellent performance in capacitors or gate dielectrics due to higher dielectric constant than its bulk counterpart while maintain its wide bandgap properties.<sup>9–11</sup>

Surface chemistry in 2D materials such as surface functionalization, chemical modification, surface synthetic chemistry and surface catalytic reactions are other prominent features for the new chemistry to improve the performance of electrochemistry and energy conversion applications using 2D architectures.<sup>12</sup> 2D materials have the ability to intercalate ions, which can provide intercalation pseudocapacitance. Moreover, 2D materials can be used as a building block for a variety of hybrid and hierarchical 2D and 3D structures. This versatility provides possibility of superstructure for high performance devices. Such composites like PANI/MoS<sub>x</sub> materials show highly enhanced capacitance behavior with long term stability without any capacitance degradation over long range of cycles.<sup>13</sup> Also the 2D structure plays a vital role in photocatalytic water splitting for producing clean energy.<sup>14</sup> Efficiency of photocatalysts strongly depends on the surface area of the photocatalysts. Various 2D<sup>1,15</sup> and thin film structure were reported to yield higher hydrogen generation. Especially porous based thin film titania<sup>16</sup> and alumina<sup>17</sup> material are

well studied for photocatalysts due to the large specific area, porosity, tunable pore size and exhibited high thermal stability. Such structural difference in the thin film (or) 2D crystals will not only improve the translation efficiency and also influence the interfacial barrier and concentration gradient. Aside from the energy related applications, the 2D platform also increasing their demand for the development of future biological prosthetic devices.<sup>18</sup> Using graphene transistors, cellular action potentials were studied as light-activated transistor conductance signals, which gives multidimensional optogenetic information. By this technique various light activated natural and artificial rhodopsins<sup>19</sup> were studied in biological tissue for research applications especially in brain science and medical fields.

With all the unique properties, devices based on 2D atomic materials already demonstrated promising performance and showed great potential for the application in electronics. On the other hand, 2D atomic materials being utilized in optical devices are comparatively limited due to the ultrathin thickness which was expected to substantially reduce the interaction volume with optical excitation. The intrinsic emission properties like fluorescence due to the direct bandgap of electronic structure are mainly well-known optical behavior for the study of 2D materials. In fact, besides fluorescence properties of 2D materials, light in combination with 2D material is useful in some optoelectronics and effectively activates or manipulates the device behaviors. Recently this novel optical method involving the interaction between light and photosensitizer was widely adopted to manipulate carrier transport behaviors via photo-induced doping in devices based on 2D materials, like graphene field effect transistors (FET). Furthermore, due to the atomically thin thickness and nearly no loss of optical transparency, 2D materials are also considered as a transparent electrode or window layer in optoelectronics such as solar cell and light emitting diode (LED). As schematically presented in the Figure 1, the phenomenon that 2D materials or 2D devices are optically manipulated by the interaction with light will be presented in this review paper through reviewing some relevant work, including some of our previous studies. The current applications using 2D materials in optoelectronics to obtain improved device properties will also be discussed.

## 2. Fluorescence of 2D Materials

**Tunable Photoluminescence of 2D Graphene Oxide.** 2D materials possess unique planar structure with an atomic layer, resulting in spectacular electronic and optical properties in comparison with their bulk structure.<sup>20–23</sup> Graphene oxide (GO) is a very good example to demonstrate its graphene sheet structure modified with oxygen functional groups which include epoxy (COC) and hydroxyl groups (COH) on the basal plane and various other types, such as carboxyl groups (COOH), carbonyl (C=O), epoxy (C-O-C) at the edges.<sup>24–26</sup> Because GO is covered by sp<sup>2</sup> and sp<sup>3</sup> carbon atoms, it exhibits interesting steady-state photoluminescence (PL) properties. PL of GO is attributed to its distinctive electronic energy transitions which originate from the energy gaps between the antibonding and the bonding molecular orbitals such as  $\sigma^* \rightarrow n$ ,  $\pi^* \rightarrow n$ , and  $\pi^* \rightarrow \pi$ .<sup>27–29</sup> Therefore, there are multiple fluorescence peaks corresponding to different electronic transitions, as shown in Figure 2a.<sup>28</sup> When these fluorescence peaks overlap with each

other, a single broad peak is observed. Besides, PL of GO can be tuned from red to blue emission by tuning the oxidation state. (Figure 2b).<sup>30</sup> By reducing the GO via a photo-thermal process, the disorder induced defect states within  $\pi^* \rightarrow \pi$  gap were gradually removed and formed numbers of isolated  $sp^2$

cluster-like domain instead. These exciton-like states formed near the conduction band edge and contributed to the blue fluorescence with narrower emission bandwidth in comparison with the wide emission red fluorescence from original GO, as depicted in Figure 2c. Chemically modified GO or rGO with n-butylamine or metal ions has also demonstrated PL emission at a range of energies.<sup>31–33</sup> The PL of GO can be affected by different pH value of the solvents.<sup>34</sup> GO exhibits a broad fluorescence band at around  $\sim 600\text{ nm} - 700\text{ nm}$  in acid conditions. With increase of pH value, the intensity of origin peak was reduced and finally, two new peaks at around  $\sim 500\text{ nm}$  emerged under basic conditions.<sup>35</sup> This pH-dependent fluorescence is believed to be caused by an excited-state proton transfer between COOH group and deprotonated carboxyl group  $\text{COO}^-$  or COOH group and COOH group in acidic or basic condition, respectively.

**Image Mapping of Graphene Oxide.** Because GO possesses an amorphous sheet structure with many defects, the PL quantum yield (QY) of GO is too low to be compared with organic fluorophores and semiconducting quantum dots.<sup>31</sup> Also, it is still hard to detect by fluorescence microscopy directly, although GO is an atomic sheet structure with large size around several micrometers to hundred micrometers.<sup>36</sup>

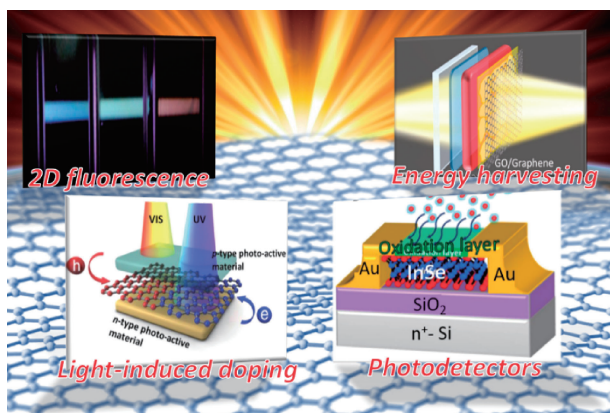


**Figure 1.** Schematically representation of scope of this review on the interaction of light and 2D atomically thin materials.

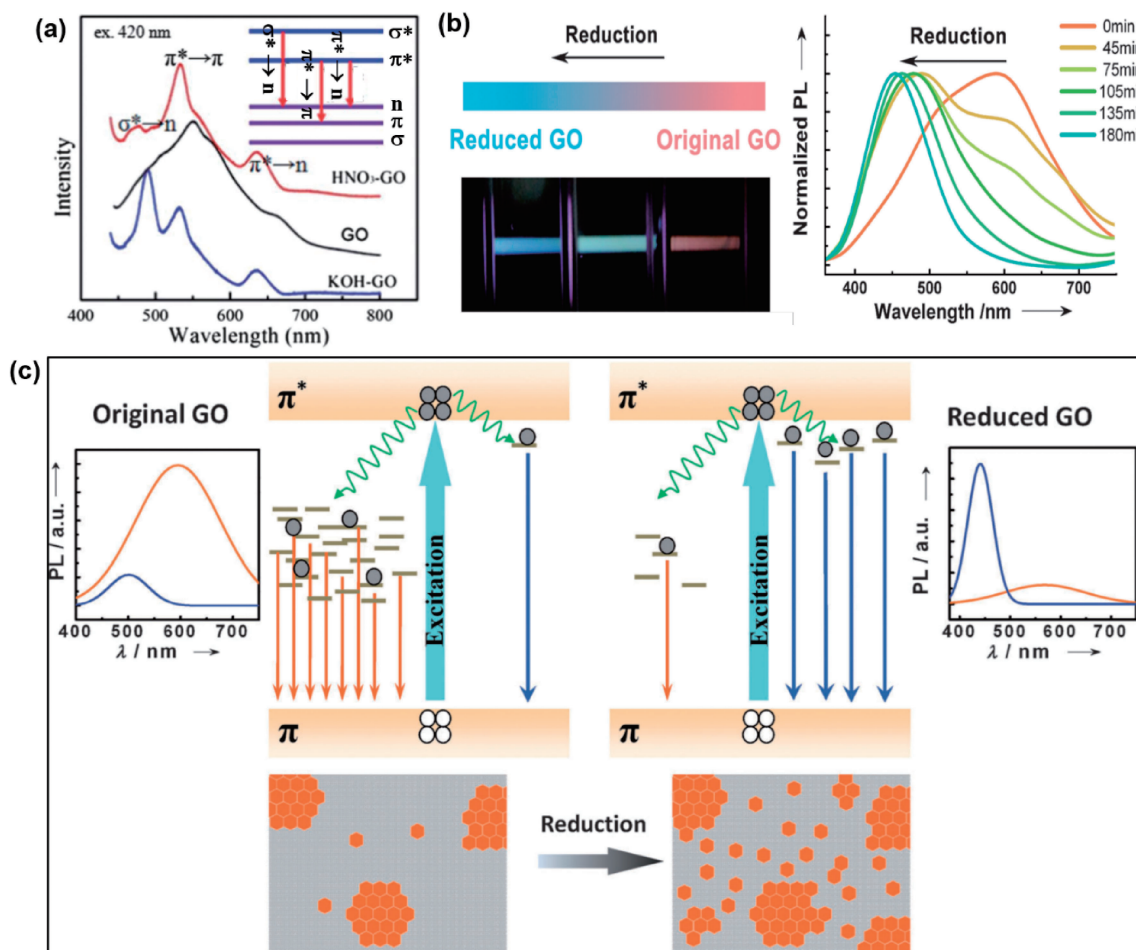


**Figure 2.** (a) PL spectra corresponding of as-synthesized GO and GO treated with KOH and  $\text{HNO}_3$ . (b) Photographs of GO PL emission tuned by photo-thermal reduction method under different illumination time (left part) and corresponding PL spectra of the GO with increase of reduction time (right part). (c) Schematic illustration of proposed PL emission mechanisms. (Reprinted from Ref. 28 and 30, copyright The Royal Society of Chemistry and John Wiley and Sons, respectively.)

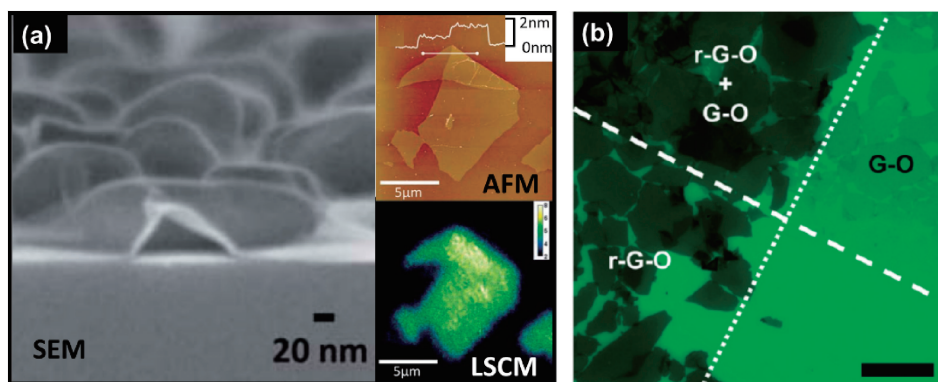


**Figure 3.** (a) Cross-sectional SEM image (upper panel), AFM and LSCM image (lower panel) of atomic layer GO thin film covered with Ag nanoparticles. (b) fluorescence quenching image of GO and reduced GO samples on glass. (Reprinted from Ref. 43 and 44, copyright The Royal Society of Chemistry and American Chemical Society, respectively.)

Current imaging techniques for graphene based sheets rely on the use of special substrates and specific techniques such as AFM, STM, SEM or TEM.<sup>37</sup> Therefore, the first priority is to enhance the PLQY of GO. One PL enhancing method is to change the chemical structure of GO itself to adjust the intrinsic PL behavior. For example, GO can be modified by surface amide formation and ring opening amination, resulting in enhancement of its PLQY.<sup>31</sup> The other feasible solution is using physical methods to enhance PL of GO without changing the chemical composition, because GO is strongly sensitive to the surrounding environment. Localized surface plasmon resonance (LSPR) is a good choice. Local electromagnetic fields adjacent to metal NPs can be enhanced by using an appropriate incident light, which excites coherent oscillation of the free electrons in the metal nanoparticles.<sup>38</sup> Many different kinds of spectroscopy, such as light absorption, PL and Raman scattering can be affected by the LSPR effect and exhibit enhancement of signal intensity.<sup>39–42</sup> Some research has shown that the luminescence of atomic layer GO film covered by Ag nanoparticles can be enhanced significantly by the near-field plasmonic effect.<sup>43</sup> Figure 3a shows that a single-layer GO flake was covered by Ag nanoparticles. From PL mapping technique, the fluorescence image of the single layer GO flake can be obtained using a laser scanning confocal microscope (LSCM) with the 405 nm laser scanned over the region (Figure 3a). The AFM and SEM images match with the fluorescence image of the GO flake signal region. The PL intensity of GO covered by Ag nanoparticles was enhanced around 30-fold in comparison with pristine one.

Graphene based sheets can also be made highly visible under a fluorescence microscope by quenching the emission from a dye coating.<sup>44</sup> The PL quenching mechanism reduces the requirement for special substrates and specific techniques. It provides an exceptional and flexible method for identifying images of fluorescent 2D materials assembled on arbitrary substrates. Figure 3b shows that a sheet topography of GO is observed on the basis of quenched dye fluorescence by GO sheet. Because of different quenching ability of GO and reduced GO, the high image contrast allowed easy identification and clearly revealed GO and reduced GO sheets. The reduced GO sheets exhibited stronger quenching ability than the GO sheets. The GO thin film demonstrated wide use in different fields, such

as energy storage,<sup>45</sup> cell culture,<sup>46</sup> sea water desalination,<sup>47</sup> biosensors<sup>48</sup> and optoelectronics.<sup>49</sup>

### 3. 2D Materials for Photodetector

In this section we briefly summarize the mechanism of photodetectors and recent photodetectors based on graphene and other 2D materials. A photodetector is a device that converts light signals into electrical signals (i.e. photocurrent or photovoltage). Basically, the photodetectors work on the mechanism of photoconductive effect, photovoltaic effect, and photothermoelectric effect. Graphene photodetectors have the advantage of ultra-broadband detection, as it can absorb ultraviolet to mid-infrared wavelengths because of their interband transitions of carriers and zero bandgap. The responsivity of graphene photodetectors is lower than traditional semiconductor based photodetectors, because the monolayer thickness of the graphene has only small optical absorption which limits the applications of graphene as a good photosensitive material. The first reported photoresponsivity of a graphene photodetector is  $\sim 0.5$  mA/W and operates at speeds greater than 500 GHz.<sup>50</sup> Later, Avouris *et al.* improved the responsivity of the graphene photodetector to 6.1 mA/W, which is 15-fold higher than previously reported.<sup>51</sup> Figure 4a illustrates the schematic view of metal-graphene-metal (MGM) photodetectors. These graphene photodetectors were fabricated on silicon wafer having 300 nm layer of silicon oxide, palladium and gold electrodes were deposited with a spacing of 1 μm. Figure 4b shows the photocurrent measurements at 1.55 μm light from a telecommunication laser of two different powers. Inset shows the diagrammatic view of the illuminated graphene device. Source-drain bias voltage measurement was performed at fixed gate voltage of  $-15$  V. The black line represents the dark current ( $I_d$ ), red and blue line represents the current after optical illumination. From the obtained results the calculated photoresponsivity of the device is  $\sim 6.1$  mA/W, still the responsivity is lower than the traditional semiconductor based photodetectors. Transition metal dichalcogenides (TMDs) is another class of layered materials with the general form of  $\text{MX}_2$ , where M stands for transition metal (Mo, W, Re, etc.) and X stands for chalcogen atoms (S, Se, or Te). These TMDs exhibit direct band gap at the monolayer due to quantum-mechanical confinement, which are suitable for optoelectronic applications. Andras Kis

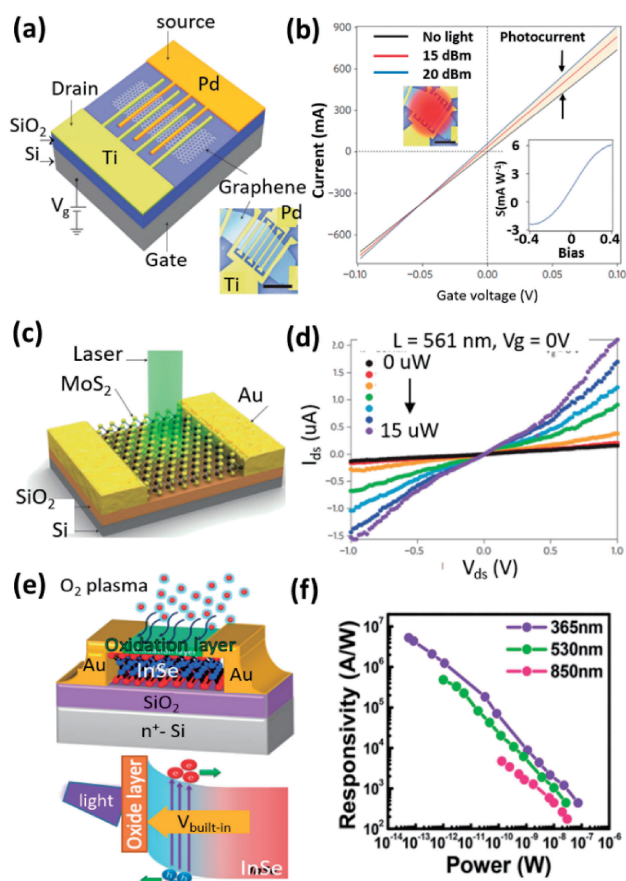


**Figure 4.** (a) Illustration of MGM photodetector (b) Source-drain bias voltage of MGM photodetector (Inset: Photoresponsivity Vs Bias voltage). (c) Diagrammatic view of MoS<sub>2</sub> photodetector. (d) Drain current Vs Drain voltage curve under dark and light conditions (561 nm wavelength at V<sub>g</sub> = 0 V). (e) InSe photodetector with SOD treatment. An enhanced built-in potential was created by the surface oxide layer as shown in the bottom panel. (f) Photoresponsivity with plasma treatment of 10 s at three different wavelengths. (Reprinted from Ref. 51 to 53, copyright Springer Nature and American Chemical Society, respectively.)

*et al.* demonstrated ultrasensitive single layer Molybdenum disulphide (MoS<sub>2</sub>) photodetector with photoresponsivity of 880 A/W at wavelength 581 nm.<sup>52</sup> Figure 4c is the three-dimensional schematic view of the monolayer MoS<sub>2</sub> photodetector under illumination of light. Figure 4d demonstrated the source-drain (I<sub>ds</sub>-V<sub>ds</sub>) measurements under dark and light illumination. When increasing the light power, the photocurrent enhanced due to greater number of electron-hole pair generation because of direct band nature of monolayer MoS<sub>2</sub>, which absorbs strong light. The responsivity reaches maximum of ~880 A/W at power of 150 pW (V<sub>ds</sub> = 8 V, V<sub>g</sub> = -70 V). Very recently, Chang *et al.* have presented an ultrahigh photoresponsivity on a 2D indium selenide (InSe) photodetector by surface oxidation doping (SOD) technique,<sup>53</sup> in which the top surface of InSe samples were mildly oxygen-doped by using oxygen plasma as schematically presented in Figure 4e. The surface doping on InSe forms an oxide/2D InSe

semiconductor heterostructure and creates a carrier concentration distribution gradient which results in vertical built-in potential along with band bending in InSe. Upon light illumination the photogenerated electron-hole pairs were separated by the internal electric field due to the carrier concentration gradient. This enhanced photogenerated carrier separation by the SOD results an ultrahigh photoresponsivity as compare to other recently reported 2D based photodetectors. Figure 4f shows the ultra-high photoresponsivity of (~5 × 10<sup>6</sup> A/W) at power 10<sup>-14</sup> W (365 nm). These results indicate that, other than graphene, semiconducting 2D materials can be a better candidate for photodetectors, yet there is still plenty of room to enhance the sensitivity.

#### 4. Photo-Induced Doping Effect in 2D Materials

Recently, a promising approach to modulate the electrical properties of a graphene transistor by using optical excitation<sup>54-56</sup> has been demonstrated, whereby photogenerated charges from a light-absorbing material can be transferred to graphene, resulting in controllable p- or n-doping processes through the use of light illumination. Compared to chemical doping, this method has the advantages of controllability and reversibility.<sup>57-59</sup> Usually the photo-induced doping process is only effective for a single type of carrier (either hole or electron), Ho *et al.* first demonstrated a dual type doping technique by illuminating the light on graphene transistor with organic-(P3HT)/graphene/inorganic(TiO<sub>x</sub>) heterostructure as showed in Figure 5a.<sup>60</sup> The band alignments of the two organic and inorganic photoactive layers with respect to graphene were able to result in charge transfer electrons or holes as presented in Figure 5b. Under illumination of light, organic P3HT or P3HT/PCBM hybrid transfer hole carriers and TiO<sub>x</sub> transfer electrons to graphene transistor. Because these two photoactive materials have distinctive optical absorption edges, graphene transistors can be controlled by using selective optical excitation with different wavelength to achieve a tunable carrier transport for n- or p-type performance. Their results presented in Figure 5c showed graphene transistor exhibited n-type transport behavior with a negative shift in charge neutral point (V<sub>CNP</sub>) to -39 V under UV irradiation; by contrast, the device exhibited a positive shift in the V<sub>CNP</sub> to 23 V when under visible light irradiation. This unique, controllable and strong photo-induced doping at graphene/TiO<sub>x</sub> heterojunction make it a potential candidate to open the bandgap of bilayer graphene through light modulation. Usually, a vertical electric field was applied to open the bandgap of bilayer graphene, via utilizing dual gate device architecture or chemical doping on single gate transistor. By using the light modulation involving the strong light and matter interaction at graphene/TiO<sub>x</sub> heterojunction, a single gate bilayer graphene transistor with device architecture shown in Figure 5d was proposed by Ho *et al.* with precisely controlled bandgap opening.<sup>61</sup> With increasing photo-induced doping concentrations (dosage of light), the V<sub>CNP</sub> of doped graphene gradually moved toward larger negative voltages. As presented in Figure 5e, the band gap value of the TiO<sub>x</sub> (top)/bilayer graphene heterostructure device is calculated to be 70 meV, with an on/off ratio around 30, as the doping concentration on the top of bilayer graphene is ≈1 × 10<sup>13</sup> cm<sup>-2</sup>. The similar photo-induced doping effect was also applied to

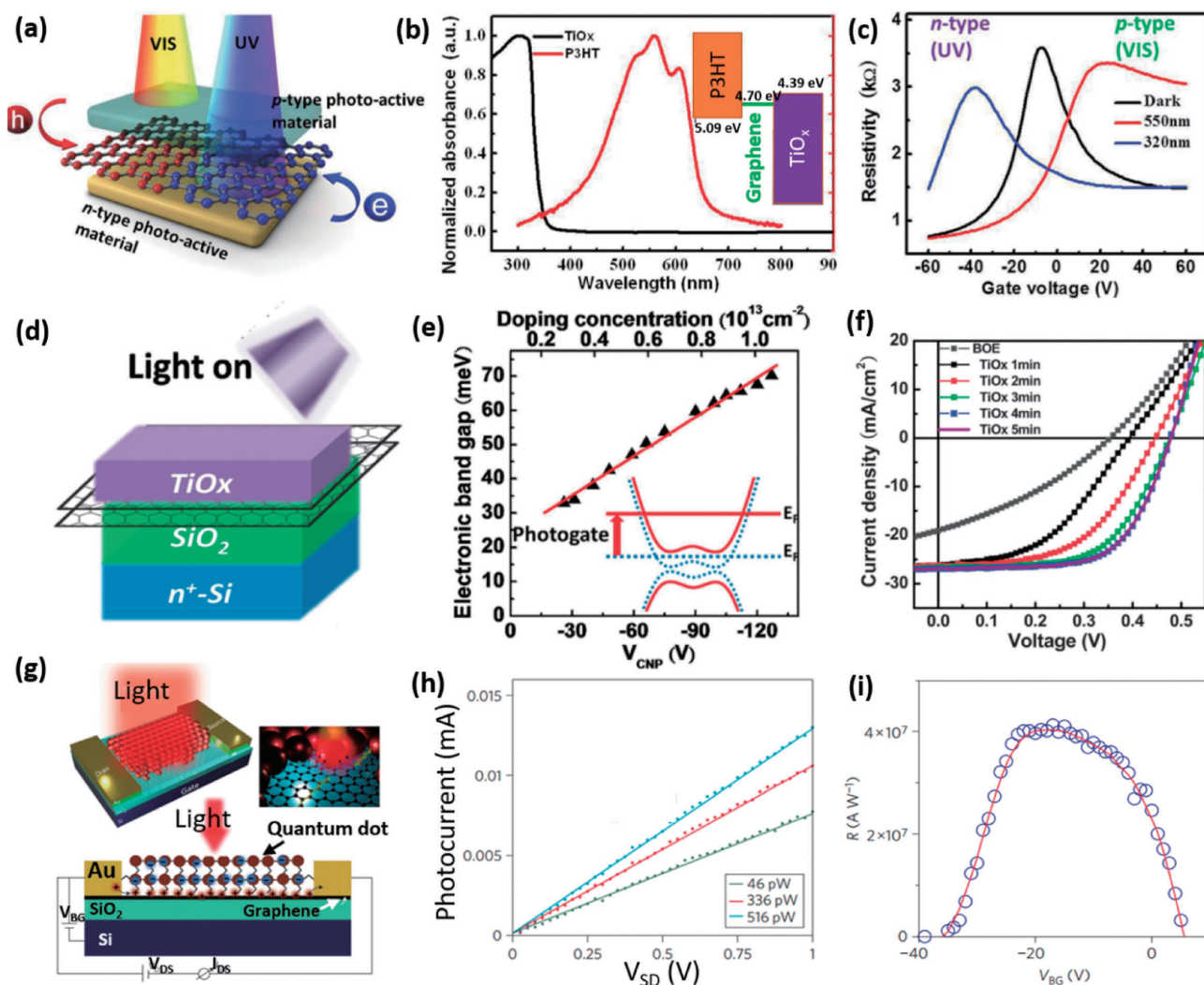


**Figure 5.** (a) Structure of organic/graphene/inorganic photo-active platform. (b) Absorption spectrum and band alignment corresponding to P3HT and  $\text{TiO}_x$ . (c) Tunable n- and p-type transport of graphene by UV and VIS light illumination, respectively. (d) Bilayer graphene transistor with  $\text{TiO}_x$  as photo-active layer. (e) Bandgap opening with various concentrations of photo-induced doping. (f) Performance of graphene/Si heterojunction solar cell.  $V_{oc}$  was improved by tuning the work function with photo-induced doping process. (g) Graphene transistor with PbS quantum dots as photo-active material. (h) Photocurrent as a function of light intensity. (i) Ultra high photoresponsivity  $\sim 10^7$  A/W. (Reprinted from Ref. 60 to 63, copyright John Wiley and Sons, The Royal Society of Chemistry and Springer Nature, respectively.)

modulate the work function of graphene by the light interaction with  $\text{TiO}_x$ . With different light dosage, the work function of graphene can be actively tuned, which was used to enlarge the built-in potential and improve the open circuit voltage of n-graphene/p-Si heterojunction solar cells, achieving a significantly improved power conversion efficiency as shown in Figure 5f.<sup>62</sup> Other materials like PbS quantum dots were also used as photo-active materials to boost the performance of graphene phototransistor. Konstantatos *et al.* showed a hybrid photodetector with high performance of PbS/graphene, in which they demonstrated high photoresponsivity of  $\sim 10^7$  A/W, ultra high gain of  $\sim 10^8$ , and high quantum efficiency.<sup>63</sup> Graphene acts as a carrier transporter, while quantum dot is the photon absorbing material as shown in Figure 5g. The photo-excited holes in the PbS quantum dots transferred to the graphene sheet and drifted toward the electrode under applied

source-drain bias ( $V_{ds}$ ), while electrons remain trapped in PbS. This resulted in a built-in field at the interface of PbS/graphene. Charge conservation in the graphene leads to hole replenishment from source, when the hole reaches the drain. By this way multiple holes circulate in the graphene sheet following a single electron-hole pair generation, which enhances the high photoconductive gain and higher responsivity as shown in Figure 5h and Figure 5i.

## 5. 2D Materials for Solar Cells and LEDs

2D materials with atomic scale thickness have been considered as promising electrode or window layer materials in future optoelectronics such as solar cells and LEDs due to the excellent physical and chemical properties. By incorporating 2D atomic materials in the conventional device architectures, it showed potentials to contribute to overcome current limita-

tions. Graphene is the material with highest expectation due to its high transparency, high electrical conductivity and mechanical flexibility. Other 2D metal oxide materials were also integrated within the device architecture to boost the device performance in different perspectives. Here we would like to introduce some published results using 2D atomic materials in photovoltaics and LEDs.

For the next generation photovoltaics, people are looking for a material that provides high power conversion efficiency while requiring low production costs to fabricate a large volume.

Organic materials such as conducting polymer and small organic molecules were one of the potential materials for this purpose in the last decade.<sup>64,65</sup> This type of material is solution processable at high throughput. Recently, another type of organic/inorganic materials with perovskite lattice structure demonstrated performance superior to conducting polymer and small molecules,<sup>66</sup> with highest power conversion efficiency over 22%, while retaining the advantages of cost-effective solution fabrication process.<sup>67</sup> Graphene, due to the high transparency and high electrical conductivity along with the full compatibility of transfer process to the solar cell solution fabrication process, was widely adopted as an electrode material for the novel photovoltaics such as polymer solar cells and perovskite solar cells. Lee *et al.* demonstrated laminating multi-layer graphene on P3HT/PCBM polymer solar cells by using thermal release tape transfer method.<sup>68</sup> A heating process at around 110 °C was used to transfer graphene layers onto P3HT/PCBM thin film while simultaneously rearranged the conformation of P3HT polymer chains and PCBM molecules to obtain a proper morphology for efficient light-to-electricity conversion. The resulting semitransparent polymer solar cell as shown in Figure 6a exhibited a promising power conversion efficiency of approximately 76% of that of the standard opaque device using an Ag metal electrode. Semi-transparent perovskite solar cells with laminated graphene electrode were demonstrated by You *et al.* by using PDMS/PMMA transfer process as shown in Figure 6b.<sup>69</sup> A thin PEDOT:PSS layer was used as an adhesion layer in the laminating process of graphene elec-

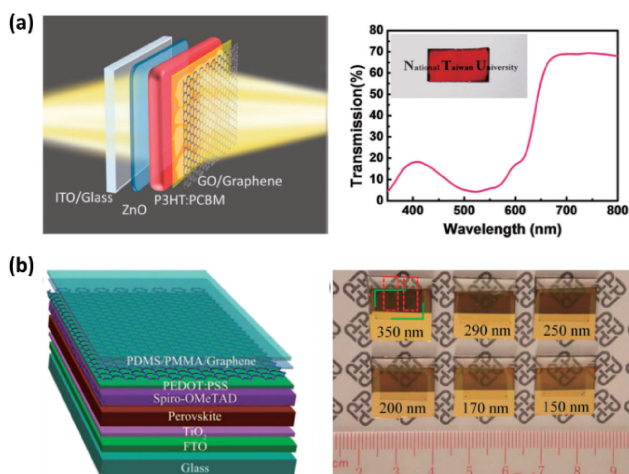


**Figure 6.** Semitransparent (a) polymer solar cell and (b) perovskite solar cell using multilayer graphene as top electrode. (Reprinted from Ref. 68 and 69, copyright American Chemical Society and John Wiley and Sons, respectively.)

trode on top of the hole transport layer (HTL, spiro-OMeTAD). Moreover, PEDOT:PSS also dopes the graphene Fermi level to get closer to the potential energy of photo-generated holes from perovskite light absorber and achieve superior hole collection efficiency. The device performance was optimized by improving the conductivity of the graphene electrodes and the contact between the top graphene electrodes and the HTL on the perovskite films. The devices with double-layer graphene electrodes show the maximum PCEs of  $12.02\% \pm 0.32\%$  and  $11.65\% \pm 0.35\%$  from the FTO and graphene sides, respectively.

Except for the application of transparent electrodes, 2D atomic materials also show excellent functionality as carrier transport layers in optoelectronics. Wang *et al.* reported a low-cost, solution-based deposition procedure utilizing nanocomposites of graphene and TiO<sub>2</sub> nanoparticles as the electron collection layers in perovskite solar cells as shown in Figure 7a.<sup>70</sup> Compared to conventional TiO<sub>2</sub> transporting layer which has to be fabricated through a high temperature annealing process at 500 °C, the composite material of graphene and TiO<sub>2</sub> was prepared at a comparatively low temperature around 150 °C while retained similar electrical conductivity to reduce the series resistance of perovskite solar cells. Another factor that improves the device performance is the reduced carrier recombination process. In the graphene/TiO<sub>2</sub> composite, most of the

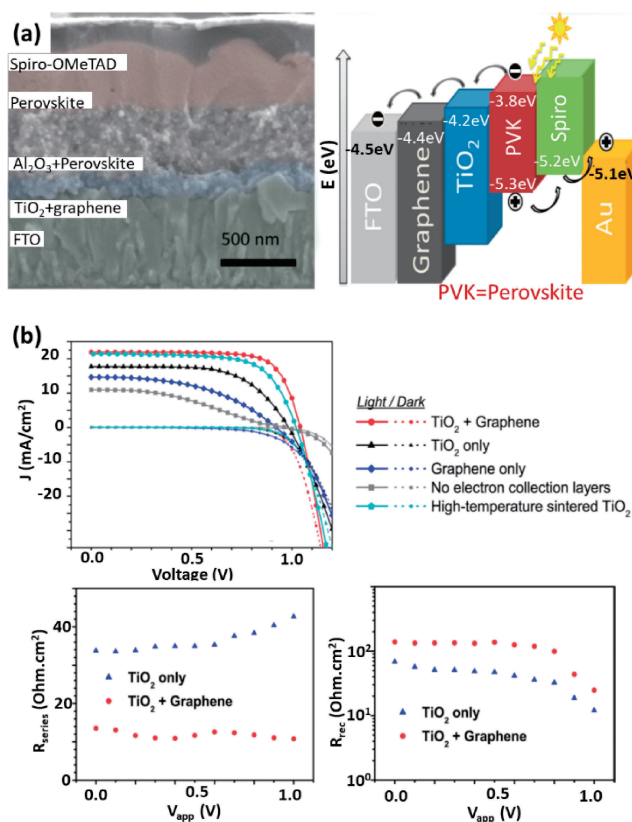


**Figure 7.** (a) Cross section SEM image and energy band alignment of perovskite solar cells using graphene/TiO<sub>2</sub> composite as ETL. (b) optimized device performance and improved series resistance and recombination resistance. (Reprinted from Ref. 70, copyright American Chemical Society.)

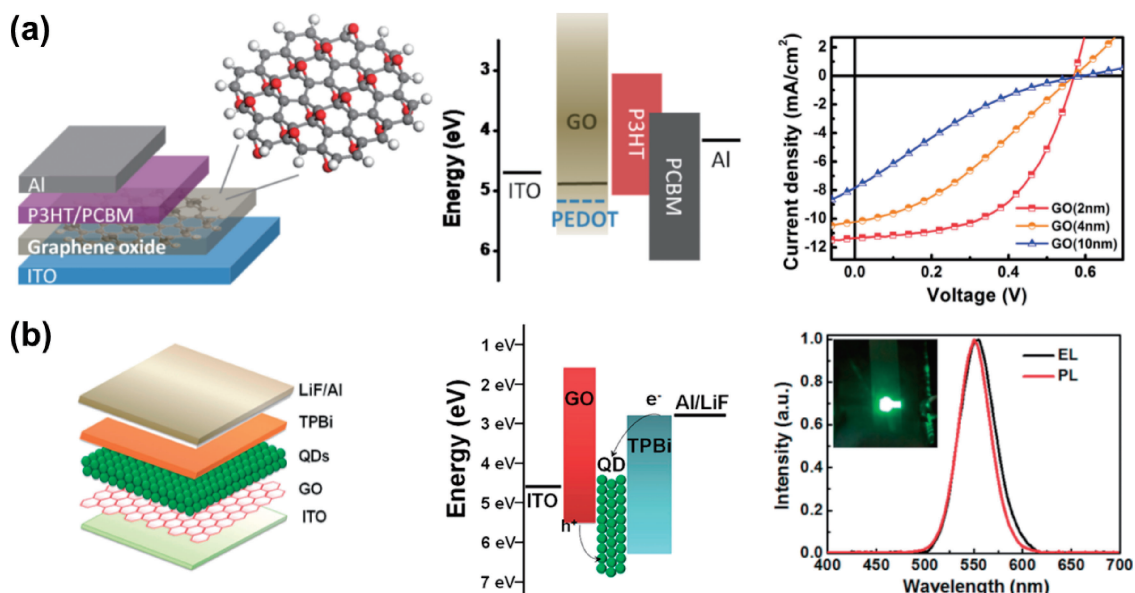


**Figure 8.** (a) The schematic of the photovoltaic device structure consisting of the following: ITO/GO/P3HT:PCBM/Al (left), related band diagram (middle) and I-V curves of the devices with different thickness of GO thin film (right). (b) the schematic of the QDLED device structure consisting of the following: ITO/GO/QDs/TPBi/LiF/Al (left), related band diagram (middle) and EL and PL of the devices with a green illumination (right). (Reprinted from Ref. 76 and 78, copyright American Chemical Society, respectively).

electron will reside on the graphene due to efficient charge transfer between graphene and  $\text{TiO}_2$ , which depleted electrons from  $\text{TiO}_2$  and leading to lower carrier recombination rate when  $\text{TiO}_2$  contacts perovskite. This in turn contributes to the increased photocurrent as presented in the Figure 7b. Biccari *et al.* also observed the utilization of graphene/ $\text{TiO}_2$  composite as electron transporting layer helped in the stabilization of perovskite tetragonal phase and improved the electron collection and perovskite crystallinity.<sup>71</sup>

The utilization of pure 2D atomic material as carrier transport layer was first accomplished by Li *et al.* by using 2nm-thick graphene oxide (GO) layer as efficient hole transport layer in polymer solar cells. Unlike graphene which has pure  $\text{sp}^2$  electronic structure and has very high electrical conductivity, the electronic structure of GO is more complex because of the presence of mixed  $\text{sp}^2$  and  $\text{sp}^3$  hybridizations.<sup>72–74</sup> From a macroscopic point of view, GO is an insulating material with very limited electrical conductivity for electrode application. However, the work function of GO ( $\sim 4.9$  eV) is slightly higher than that of pristine graphene (4.6 eV),<sup>75</sup> which is more compatible to the valence band position of polymer based and perovskite based photovoltaic materials.<sup>75</sup> Many reports found that atomic layer GO thin film performed well in mediating the hole transport behavior between electrode and active materials in solar cells and LED applications. The first report is using GO with a thickness of 2 nm as HTM for polymer solar cell to replace traditional PEDOT:PSS HTM with the following device structure: ITO/PEDOT:PSS/P3HT:PCBM/Al (Figure 8a).<sup>76</sup> The device based on GO HTM exhibited a competitive power conversion efficiency  $\sim 3.5\%$  in comparison with typical device performance of ITO/PEDOT:PSS/P3HT:PCBM/Al  $\sim 3.6\%$ . With the high LUMO level, thin GO layer can effectively block electrons from active layer to ITO

electrode and prevented the electron-hole recombination. Meanwhile, photo-generated holes from active layer can tunnel through atomically thin insulating layer of GO toward ITO electrode for photocurrent generation. Reduced GO with finite conductivity was also applied as a HTL to guarantee efficient and stable  $\text{CH}_3\text{NH}_3\text{PbI}_3$  perovskite solar cells.<sup>77</sup> The resultant solar cell with a planar configuration of ITO/RGO/ $\text{CH}_3\text{NH}_3\text{PbI}_3$ /PC<sub>61</sub>BM/bathocuproine (BCP)/Ag exhibits improved device efficiency (maximum PCE of 10.8%) with higher reproducibility and stability than those of the reference devices using conventional PEDOT:PSS and GO HTMs. Wang *et al.* used solution processable GO thin film as the anode interfacial layer in quantum dot light emitting diodes (QD-LEDs).<sup>78</sup> The structure of QD-LED devices consists of ITO/GO/QDs/TPBi/LiF/Al by employing a layer-by-layer assembled deposition technique (Figure 8b). The best luminescence performance of the device achieved to  $165 \text{ cd m}^{-2}$  at  $232 \text{ mA cm}^{-2}$ , operated at an applied voltage of 8 V. The GO can also be applied in organic light-emitting diodes (OLEDs). The device (ITO/GO/TPD/Alq<sub>3</sub>/LiF/Al) exhibited a high luminance of over  $53000 \text{ cd m}^{-2}$  operated at only 10 V.<sup>79</sup>

Recently, titania ( $\text{Ti}_{1-\delta}\text{O}_2$ ) with 2D lattice structure was also used as an efficient electron transport layer (ETL) in perovskite solar cells.<sup>80</sup> The most popular ETL in the high-performance perovskite solar cells is the inorganic compact  $\text{TiO}_2$  (c- $\text{TiO}_2$ ) layer. However, high-temperature sintering ( $450\text{--}550^\circ\text{C}$ ) is usually required to prepare the c- $\text{TiO}_2$  layers, which may cause the limitation of perovskite solar cells being deposited on thermally sensitive substrates. Chen *et al.* demonstrated the utilization of novel 2D atomic sheets of titania as a building block for a new type of atomic stacking transporting layer (ASTL) in perovskite solar cells by using a solution process at room temperature. As presented in Figure 9a, the 2D titania

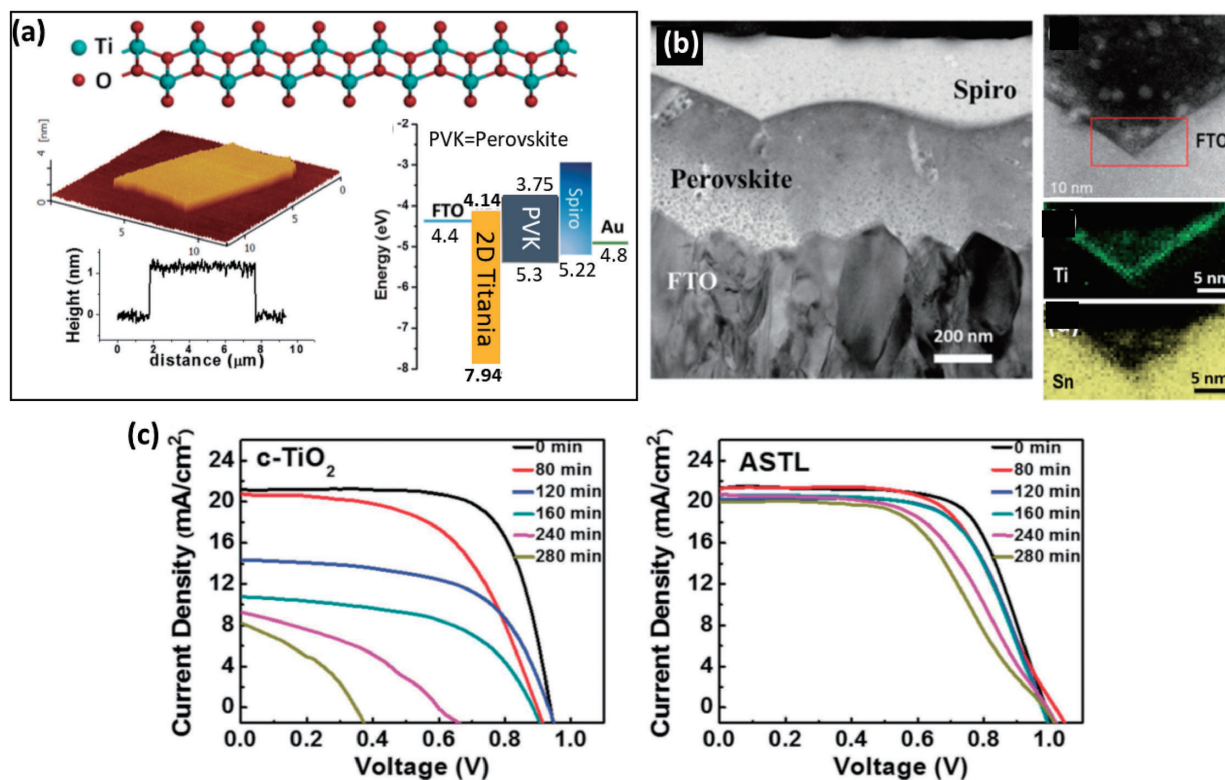


**Figure 9.** (a) Lattice structure of 2D titania with thickness of 1 nm and lateral size of 10 to 20  $\mu\text{m}$ . It was used as an electron transport layer in perovskite solar cells. (b) TEM cross section image and EELS mapping shows the thickness of 2D titania is around 3 nm. (c) solar cell stability under UV light excitation based on conventional c-TiO<sub>2</sub> and 2D titania ASTL as ETL material. (Reprinted from Ref. 80, copyright John Wiley and Sons.)

atomic structural arrangement is a 2D slab where TiO<sub>6</sub> octahedra are edge linked in a lepidocrocite-type 2D lattice. The exfoliated 2D titania has typical thickness around 1 nm and lateral dimension around 10 to 20  $\mu\text{m}$  for monolayer of 2D titania. Due to the n-type properties of 2D titania, it was used as an electron transport layer between FTO electrode and perovskite layer. From the cross-sectional TEM image and electron energy loss spectroscopy (EELS) mapping of Ti atom signals (Figure 9b, right-middle panel), the ASTL has excellent conformity over the FTO substrate surface, providing nearly intact junctions with the upper part of perovskite active layer and lower part of FTO substrate. The average thickness of the ASTL of 2D titania is estimated to be around 3 nm, corresponding to the average thickness of three layers of titania atomic sheets. The solar cell fabricated based on the 2D titania provided a promising power conversion efficiency of 15.24% with merely 3 layers of 2D titania. The resulting performance is compatible to the conventional perovskite solar cells using high temperature processed c-TiO<sub>2</sub> as ETL with a thickness around 200 nm. Furthermore, because the intrinsic 2D titania atomic sheets consist of negligible (or very low) oxygen vacancies, so that the photocatalytic reaction of the perovskite film deposited on 2D titania atomic sheets under UV excitation is not effective. Therefore, as shown in Figure 9c, perovskite solar cells consisting of 2D titania ASTL exhibited excellent UV stability on the device performance as compared to that consisting of a conventional c-TiO<sub>2</sub> ETL due to the unique properties of negligible oxygen vacancy of 2D titania atomic sheets.

## 6. Conclusion and Perspective

Atomically thin 2D materials has already showed great potential in electronics due to the excellent electrical properties, such as high mobility and high conductivity. The outstanding performance in electronics underrated the potential of 2D materials to be influenced by light. In this review article, we shed light on the interactions of 2D materials with photons, through fluorescence, light-induced photo-doing effect, and the applications utilized in the next generation solar cells and LEDs. These results represent that light is handy to functionalize 2D materials and 2D devices. With proper combination of photosensitizer, photons are greatly effective to manipulate the electrical transport behaviors, showing a unique advantage compared to the techniques used to control the currently widely-used bulk semiconductors. On the other hand, with atomic thickness and unique electronic structure, 2D materials can be a useful building block to improve the performance of optoelectronics and can be an assistant to overcome the current device limitations.

This work is supported by Ministry of Science and Technology (MOST), Taiwan (Project No. 105-2112-M-038-001-MY3, 106-2113-M-029-006-MY2 and 106-2622-E-038-001-CC2) The authors would like to express thanks for valuable discussion with Prof. Chun-Wei Chen at Department of Material Science and Engineering, National Taiwan University.

## References

- # These authors contributed equally.
- 1 C. Tan, X. Cao, X.-J. Wu, Q. He, J. Yang, X. Zhang, J. Chen, W. Zhao, S. Han, G.-H. Nam, *Chem. Rev.* **2017**, *117*, 6225.
  - 2 A. J. Mannix, B. Kiraly, M. C. Hersam, N. P. Guisinger, *Nat Rev Chem.* **2017**, *1*, 0014.
  - 3 D. Akinwande, C. J. Brennan, J. S. Bunch, P. Egberts, J. R. Felts, H. Gao, R. Huang, J.-S. Kim, T. Li, Y. Li, K. M. Liechti, N. Lu, H. S. Park, E. J. Reed, P. Wang, B. I. Yakobson, T. Zhang, Y.-W. Zhang, Y. Zhou, Y. Zhu, *Extreme Mech. Lett.* **2017**, *13*, 42.
  - 4 K. Novoselov, A. Mishchenko, A. Carvalho, A. H. C. Neto, *Science* **2016**, *353*, aac9439.
  - 5 Y. Tobe, K. Tahara, S. De Feyter, *Bull. Chem. Soc. Jpn.* **2016**, *89*, 1277.
  - 6 A. H. Castro Neto, F. Guinea, N. M. R. Peres, K. S. Novoselov, A. K. Geim, *Rev. Mod. Phys.* **2009**, *81*, 109.
  - 7 F. Bonaccorso, Z. Sun, T. Hasan, A. Ferrari, *Nat. Photonics* **2010**, *4*, 611.
  - 8 K. F. Mak, C. Lee, J. Hone, J. Shan, T. F. Heinz, *Phys. Rev. Lett.* **2010**, *105*, 136805.
  - 9 B.-W. Li, M. Osada, Y. Ebina, K. Akatsuka, K. Fukuda, T. Sasaki, *ACS Nano* **2014**, *8*, 5449.
  - 10 M. Osada, T. Sasaki, *Adv. Mater.* **2012**, *24*, 210.
  - 11 M. Osada, T. Sasaki, *J. Mater. Chem.* **2009**, *19*, 2503.
  - 12 Q. Fu, X. Bao, *Chem. Soc. Rev.* **2017**, *46*, 1842.
  - 13 Y. Wang, C. C. Mayorga-Martinez, M. Pumera, *Bull. Chem. Soc. Jpn.* **2017**, *90*, 847.
  - 14 M. Lozada-Hidalgo, S. Zhang, S. Hu, V. G. Kravets, F. J. Rodriguez, A. Berdyugin, A. Grigorenko, A. K. Geim, *Nat. Nanotechnol.* **2018**. doi:10.1038/s41565-017-0051-5.
  - 15 A. H. Khan, S. Ghosh, B. Pradhan, A. Dalui, L. K. Shrestha, S. Acharya, K. Ariga, *Bull. Chem. Soc. Jpn.* **2017**, *90*, 627.
  - 16 Y.-T. Liao, C.-W. Huang, C.-H. Liao, J. C.-S. Wu, K. C.-W. Wu, *Appl. Energy* **2012**, *100*, 75.
  - 17 X. Jiang, N. Suzuki, B. P. Bastakoti, K. C.-W. Wu, Y. Yamauchi, *Chem.—Asian J.* **2012**, *7*, 1713.
  - 18 B. L. Li, M. I. Setyawati, L. Chen, J. Xie, K. Ariga, C.-T. Lim, S. Garaj, D. T. Leong, *ACS Appl. Mater. Interfaces* **2017**, *9*, 15286.
  - 19 K. Inoue, *Bull. Chem. Soc. Jpn.* **2016**, *89*, 1416.
  - 20 K. Novoselov, D. Jiang, F. Schedin, T. J. Booth, V. V. Khotkevich, S. V. Morozov, A. Geim, *Proc. Natl. Acad. Sci. U.S.A.* **2005**, *102*, 10451.
  - 21 P. Avouris, Z. Chen, V. Perebeinos, *Nat. Nanotechnol.* **2007**, *2*, 605.
  - 22 Y. Sun, Q. Wu, G. Shi, *Energy Environ. Sci.* **2011**, *4*, 1113.
  - 23 S. Z. Butler, S. M. Hollen, L. Cao, Y. Cui, J. A. Gupta, H. R. Gutiérrez, T. F. Heinz, S. S. Hong, J. Huang, A. F. Ismach, E. Johnston-Halperin, M. Kuno, V. V. Plashnitsa, R. D. Robinson, R. S. Ruoff, S. Salahuddin, J. Shan, L. Shi, M. G. Spencer, M. Terrones, W. Windl, J. E. Goldberger, *ACS Nano* **2013**, *7*, 2898.
  - 24 D. R. Dreyer, S. Park, C. W. Bielawski, R. S. Ruoff, *Chem. Soc. Rev.* **2010**, *39*, 228.
  - 25 Y. Zhu, S. Murali, W. Cai, X. Li, J. W. Suk, J. R. Potts, R. S. Ruoff, *Adv. Mater.* **2010**, *22*, 3906.
  - 26 M. J. Allen, V. C. Tung, R. B. Kaner, *Chem. Rev.* **2010**, *110*, 132.
  - 27 G. Eda, Y.-Y. Lin, C. Mattevi, H. Yamaguchi, H.-A. Chen, I.-S. Chen, C.-W. Chen, M. Chhowalla, *Adv. Mater.* **2010**, *22*, 505.
  - 28 M. Li, S. K. Cushing, X. Zhou, S. Guo, N. Wu, *J. Mater. Chem.* **2012**, *22*, 23374.
  - 29 C.-H. Chuang, Y.-F. Wang, Y.-C. Shao, Y.-C. Yeh, D.-Y. Wang, C.-W. Chen, J. W. Chiou, S. C. Ray, W. F. Pong, L. Zhang, J. F. Zhu, J. H. Guo, *Sci. Rep.* **2014**, *4*, 4525.
  - 30 C.-T. Chien, S.-S. Li, W.-J. Lai, Y.-C. Yeh, H.-A. Chen, I.-S. Chen, L.-C. Chen, K.-H. Chen, T. Nemoto, S. Isoda, M. Chen, T. Fujita, G. Eda, H. Yamaguchi, M. Chhowalla, C.-W. Chen, *Angew. Chem., Int. Ed.* **2012**, *51*, 6662.
  - 31 Q. Mei, K. Zhang, G. Guan, B. Liu, S. Wang, Z. Zhang, *Chem. Commun.* **2010**, *46*, 7319.
  - 32 Z. X. Gan, S. J. Xiong, X. L. Wu, C. Y. He, J. C. Shen, P. K. Chu, *Nano Lett.* **2011**, *11*, 3951.
  - 33 D.-Y. Wang, D.-W. Wang, H.-A. Chen, T.-R. Chen, S.-S. Li, Y.-C. Yeh, T.-R. Kuo, J.-H. Liao, Y.-C. Chang, W.-T. Chen, S.-H. Wu, C.-C. Hu, C.-W. Chen, C.-C. Chen, *Carbon* **2015**, *82*, 24.
  - 34 C. Galande, A. D. Mohite, A. V. Naumov, W. Gao, L. Ci, A. Ajayan, H. Gao, A. Srivastava, R. B. Weisman, P. M. Ajayan, *Sci. Rep.* **2011**, *1*, 85.
  - 35 S. K. Cushing, M. Li, F. Huang, N. Wu, *ACS Nano* **2014**, *8*, 1002.
  - 36 L. J. Cote, F. Kim, J. Huang, *J. Am. Chem. Soc.* **2009**, *131*, 1043.
  - 37 X. Huang, Z. Yin, S. Wu, X. Qi, Q. He, Q. Zhang, Q. Yan, F. Boey, H. Zhang, *Small* **2011**, *7*, 1876.
  - 38 K. L. Kelly, E. Coronado, L. L. Zhao, G. C. Schatz, *J. Phys. Chem. B* **2003**, *107*, 688.
  - 39 O. Kulakovich, N. Strekal, A. Yaroshevich, S. Maskevich, S. Gaponenko, I. Nabiev, U. Woggon, M. Artemyev, *Nano Lett.* **2002**, *2*, 1449.
  - 40 K. Shimizu, W. Woo, B. Fisher, H. Eisler, M. G. Bawendi, *Phys. Rev. Lett.* **2002**, *89*, 117401.
  - 41 K. Okamoto, I. Niki, A. Shvartser, Y. Narukawa, T. Mukai, A. Scherer, *Nat. Mater.* **2004**, *3*, 601.
  - 42 K. Ray, R. Badugu, J. R. Lakowicz, *J. Am. Chem. Soc.* **2006**, *128*, 8998.
  - 43 Y. Wang, S.-S. Li, Y.-C. Yeh, C.-C. Yu, H.-L. Chen, F.-C. Li, Y.-M. Chang, C.-W. Chen, *Nanoscale* **2013**, *5*, 1687.
  - 44 J. Kim, L. J. Cote, F. Kim, J. Huang, *J. Am. Chem. Soc.* **2010**, *132*, 260.
  - 45 M. D. Stoller, S. Park, Y. Zhu, J. An, R. S. Ruoff, *Nano Lett.* **2008**, *8*, 3498.
  - 46 W. C. Lee, C. H. Y. X. Lim, H. Shi, L. A. L. Tang, Y. Wang, C. T. Lim, K. P. Loh, *ACS Nano* **2011**, *5*, 7334.
  - 47 E. N. Wang, R. Karnik, *Nat. Nanotechnol.* **2012**, *7*, 552.
  - 48 C. Shan, H. Yang, J. Song, D. Han, A. Ivaska, L. Niu, *Anal. Chem.* **2009**, *81*, 2378.
  - 49 G. Eda, M. Chhowalla, *Adv. Mater.* **2010**, *22*, 2392.
  - 50 F. Xia, T. Mueller, Y. Lin, A. Valdes-Garcia, P. Avouris, *Nat. Nanotechnol.* **2009**, *4*, 839.
  - 51 T. Mueller, F. Xia, P. Avouris, *Nat. Photonics* **2010**, *4*, 297.
  - 52 O. Lopez-Sanchez, D. Lembke, M. Kayci, A. Radenovic, A. Kis, *Nat. Nanotechnol.* **2013**, *8*, 497.
  - 53 Y.-R. Chang, P.-H. Ho, C.-Y. Wen, T.-P. Chen, S.-S. Li, J.-Y. Wang, M.-K. Li, C.-A. Tsai, R. Sankar, W.-H. Wang, P.-W. Chiu, F.-C. Chou, C.-W. Chen, *ACS Photonics* **2017**, *4*, 2930.
  - 54 S.-Y. Chen, Y.-Y. Lu, F.-Y. Shih, P.-H. Ho, Y.-F. Chen, C.-W. Chen, Y.-T. Chen, W.-H. Wang, *Carbon* **2013**, *63*, 23.
  - 55 D. Zhang, L. Gan, Y. Cao, Q. Wang, L. Qi, X. Guo, *Adv. Mater.* **2012**, *24*, 2715.
  - 56 W. Guo, S. Xu, Z. Wu, N. Wang, M. M. T. Loy, S. Du,

*Small* **2013**, *9*, 3031.

57 J. M. Englert, C. Dotzer, G. Yang, M. Schmid, C. Papp, J. M. Gottfried, H.-P. Steinrück, E. Spiecker, F. Hauke, A. Hirsch, *Nat. Chem.* **2011**, *3*, 279.

58 S.-Y. Chen, P.-H. Ho, R.-J. Shiue, C.-W. Chen, W.-H. Wang, *Nano Lett.* **2012**, *12*, 964.

59 M. Lafkioti, B. Krauss, T. Lohmann, U. Zschieschang, H. Klauk, K. v. Klitzing, J. H. Smet, *Nano Lett.* **2010**, *10*, 1149.

60 P.-H. Ho, S.-S. Li, Y.-T. Liou, C.-Y. Wen, Y.-H. Chung, C.-W. Chen, *Adv. Mater.* **2015**, *27*, 282.

61 P.-H. Ho, C.-H. Chen, F.-Y. Shih, Y.-R. Chang, S.-S. Li, W.-H. Wang, M.-C. Shih, W.-T. Chen, Y.-P. Chiu, M.-K. Li, Y.-S. Shih, C.-W. Chen, *Adv. Mater.* **2015**, *27*, 7809.

62 P.-H. Ho, W.-C. Lee, Y.-T. Liou, Y.-P. Chiu, Y.-S. Shih, C.-C. Chen, P.-Y. Su, M.-K. Li, H.-L. Chen, C.-T. Liang, C.-W. Chen, *Energy Environ. Sci.* **2015**, *8*, 2085.

63 G. Konstantatos, M. Badioli, L. Gaudreau, J. Osmond, M. Bernechea, F. P. G. de Arquer, F. Gatti, F. H. L. Koppens, *Nat. Nanotechnol.* **2012**, *7*, 363.

64 Y.-J. Cheng, S.-H. Yang, C.-S. Hsu, *Chem. Rev.* **2009**, *109*, 5868.

65 Y. Sun, G. C. Welch, W. L. Leong, C. J. Takacs, G. C. Bazan, A. J. Heeger, *Nat. Mater.* **2012**, *11*, 44.

66 T. Noma, Y. Zhang, Z. Yao, M. Iwamoto, H. Lin, *Chem. Lett.* **2017**, *46*, 1105.

67 W. S. Yang, B.-W. Park, E. H. Jung, N. J. Jeon, Y. C. Kim, D. U. Lee, S. S. Shin, J. Seo, E. K. Kim, J. H. Noh, S. I. Seok, *Science* **2017**, *356*, 1376.

68 Y.-Y. Lee, K.-H. Tu, C.-C. Yu, S.-S. Li, J.-Y. Hwang, C.-C. Lin, K.-H. Chen, L.-C. Chen, H.-L. Chen, C.-W. Chen, *ACS Nano* **2011**, *5*, 6564.

69 P. You, Z. Liu, Q. Tai, S. Liu, F. Yan, *Adv. Mater.* **2015**, *27*, 3632.

70 J. T.-W. Wang, J. M. Ball, E. M. Barea, A. Abate, J. A. Alexander-Webber, J. Huang, M. Saliba, I. Mora-Sero, J. Bisquert, H. J. Snaith, R. J. Nicholas, *Nano Lett.* **2014**, *14*, 724.

71 F. Biccari, F. Gabelloni, E. Burzi, M. Gurioli, S. Pescetelli, A. Agresti, A. E. Del Rio Castillo, A. Ansaldo, E. Kymakis, F. Bonaccorso, A. D. Carlo, A. Vinattieri, *Adv. Energy Mater.* **2017**, *7*, 171349.

72 C. Mattevi, G. Eda, S. Agnoli, S. Miller, K. A. Mkhoyan, O. Celik, D. Mastrogiovanni, G. Granozzi, E. Garfunkel, M. Chhowalla, *Adv. Funct. Mater.* **2009**, *19*, 2577.

73 G. Eda, C. Mattevi, H. Yamaguchi, H. Kim, M. Chhowalla, *J. Phys. Chem. C* **2009**, *113*, 15768.

74 G. Eda, G. Fanchini, M. Chhowalla, *Nat. Nanotechnol.* **2008**, *3*, 270.

75 Y.-J. Yu, Y. Zhao, S. Ryu, L. E. Brus, K. S. Kim, P. Kim, *Nano Lett.* **2009**, *9*, 3430.

76 S.-S. Li, K.-H. Tu, C.-C. Lin, C.-W. Chen, M. Chhowalla, *ACS Nano* **2010**, *4*, 3169.

77 J.-S. Yeo, R. Kang, S. Lee, Y.-J. Jeon, N. Myoung, C.-L. Lee, D.-Y. Kim, J.-M. Yun, Y.-H. Seo, S.-S. Kim, *Nano Energy* **2015**, *12*, 96.

78 D.-Y. Wang, I.-S. Wang, I.-S. Huang, Y.-C. Yeh, S.-S. Li, K.-H. Tu, C.-C. Chen, C.-W. Chen, *J. Phys. Chem. C* **2012**, *116*, 10181.

79 S. Shi, V. Sadhu, R. Moubah, G. Schmerber, Q. Bao, S. R. P. Silva, *J. Mater. Chem. C* **2013**, *1*, 1708.

80 T.-P. Chen, C.-W. Lin, S.-S. Li, Y.-H. Tsai, C.-Y. Wen, W. J. Lin, F.-M. Hsiao, Y.-P. Chiu, K. Tsukagoshi, M. Osada, T. Sasaki, C.-W. Chen, *Adv. Energy Mater.* **2018**, *8*, 1701722.